Ultrafast electron dynamics in metals under laser irradiation

Andrey V. Lugovskoy* and Igor Bray
Electronic Structure of Materials Centre, The Flinders University of South Australia, G.P.O. Box 2100, Adelaide 5001, Australia
(Received 15 October 1998)

The evolution of the electron distribution in a metal irradiated by an ultrashort laser pulse is described on the basis of numerical solution of the equation for the one-particle density matrix. The excitation mechanism is attributed to the laser quanta absorption in electron collisions with both longitude and transverse-acoustic phonons. It is shown that the absorption is mainly determined by the umklapp processes. The electron relaxation is due to electron-electron collisions taken into account using the relaxation-time approximation. The agreement with the experiment of Fann *et al.* [Phys. Rev. B **46**, 13 592 (1992)] is good.
[S0163-1829(99)04625-1]

I. INTRODUCTION

Investigation of ultrafast electron dynamics and transport in solids, particularly in metals, has drawn much attention in the last few years.[1–5] This interest is associated with the progress of the femtosecond laser technique. The use of modern optical methods allows a direct characteristic rate measurement of electron processes,[6–10] and direct monitoring of the nonequilibrium electron distribution in real time.[11,12] These studies provide valuable information for testing and further development of the solid-state theory. In addition, the results of these investigations are needed in a variety of technological applications, for example microelectronics, surface photochemistry, and laser technology.

The energy transport in a metal, subjected to an ultrashort laser pulse, is widely treated within the two-temperature model.[13,14] It describes the energy exchange between the electron gas and the lattice on the basis of the coupled equations for the electron and lattice temperatures. This model assumes that electrons first thermalize among themselves and subsequently lose energy to the lattice.

It was thought for a long time, due to the successful application of the two-temperature model, that the laser behaved as a pure thermal source. Recently it has been shown experimentally that thermalization of electrons and energy transfer from the electrons to the lattice are not separated in time during irradiation[8,15] and the electron distribution is nonequilibrium[12,16] (here and further the nonequilibrium electron distribution means the electron distribution averaged over the laser period).

The investigations conducted over the last decade have significantly promoted our understanding of the laser initiated electron processes in metals. They also revealed some problems like discrepancy in the experimental and the Fermi-liquid theory calculated electron-electron scattering rates,[17–19] and ''above threshold ionization'' spectrum of electrons emitted from the metal under surprisingly low intensities.[20–22] In our opinion, the key to explaining these phenomena lies in the understanding of the nonequilibrium dynamics of electrons in the laser irradiated metal. This area of research has been relatively unexplored.

The physical picture of the laser action on the electrons in the metal is quite simple. Optical excitation of a metal produces electrons with energies far above the Fermi level. The excitation is balanced by various relaxation processes. The complexity of this problem arises through a large number of possible excitation and relaxation channels including interband transitions, laser-stimulated collisions of electrons with phonons, and e-e scattering. Fann *et al.*[11,12] have experimentally demonstrated how the nonequilibrium electron distribution evolves in time. It was shown that the laser irradiation leads to a nearly flat energy distribution extending from the Fermi level ϵ_F to the energy $\epsilon_F+\hbar\omega$ (ω is the laser frequency) which disappears for the characteristic e-e relaxation time when the radiation is turned off.

In this work we will consider the case where the laser frequency is sufficiently small to excite interband transitions, as in the experiments of Fann *et al.*[11,12] Then, the interaction of the laser field with the electrons in the metal is mainly mediated by phonons. To the best of our knowledge, the first theoretical treatment of electron dynamics in a metal under laser irradiation with consideration of quantum effects has been conducted by Gurzhi.[23] In the first-order approximation, of the laser intensity, he derived the relation for the electron-phonon (e-p) collision integral modified by the presence of the field and applied it to the analysis of infrared absorptivity of metals.[24] This e-p collision integral did not account for electron transitions with absorption or emission of the field photons which are of the second order in the laser intensity. Subsequently, the field modified e-p collision integral has been derived by several authors where these processes have been taken into account.[25–27]

In metals, formation of the nonequilibrium electron distribution was considered by Zinoviev and Lugovskoy[28] and Lugovskoy, Usmanov, and Zinoviev.[29] The interaction of electrons with a laser field was described phenomenologically via intraband transitions linking the electronic states separated by the value equal to some integral number of laser quanta. Recently, this approach has been generalized[27] using the formalism for one-particle density matrix. This allowed us to relate the phenomenological photon absorption rate[29] with the e-p collision rate.

The numerical solution of the Boltzmann equation for the electrons in a metal under pulsed laser irradiation was reported by Sun *et al.*[30] In this work, the interaction of the electrons with the field is also considered phenomenologi-

cally while the *e-e* relaxation is treated exactly.

Formation of the nonequilibrium electron distribution in a metal has also been considered recently in the work by Bejan and Raşeev.[31] They neglect laser quantum absorption in *e-p* collisions and try to explain the production of the athermal distribution in the experiment of Fann *et al.*[12] as a consequence of resonant dipole transitions between two levels ϵ_i and $\epsilon_f=\epsilon_i+\hbar\omega$. However, we shall argue that this mechanism is not appropriate for metals.

In this paper our aim is to explain the experiment of Fann *et al.* on the basis of the theory reported by Lugovskoy, Usmanov, and Zinoviev.[27] We find that much improved agreement with the experimental data is provided by the accounting of umklapp *e-p* collisions. Our calculations show that, for hot electrons, the umklapp processes sufficiently dominate the normal collisions. Moreover, the calculated *e-p* collision rate, not modified by the field, is generally higher than the *e-e* scattering rate in the energy region where ''above threshold ionization'' electrons have been detected. This fact may explain the recent findings by Luan *et al.*,[20] Farkas, Toth, and Kohazi-Kis,[21] and Farkas *et al.*[22]

The structure of the work is as follows. In Sec. II we generalize the model[27] to include *e-p* umklapp collisions. Here we derive the equation for the nonequilibrium distribution function. Section III is devoted to the calculation of the *e-e* scattering and *e-p* collision rates. The solution of the kinetic equation in the region from ϵ_F to $\epsilon_F+\hbar\omega$ is presented in Sec. IV. Section V summarizes the results of the present work.

II. MODEL

Let an ultrashort laser pulse fall on a flat metal surface. Some part of the radiation reflects from the surface and another part $\mathbf{E}(t)=\mathbf{E}_0(t)\sin\omega t$ is absorbed producing hot electrons in a thin skin layer of depth ~ 15 nm. The absorbed energy is then redistributed among electrons due to *e-e* collisions and transfer to the lattice through *e-p* collisions. The energy from the skin layer can also be lost by diffusion of hot electrons out of this region.

We assume that no interband transitions from *d* bands to the *sp* band occur, that is, the laser frequency and intensity are sufficiently small. Here we also neglect the ballistic transport effects and consider the electron distribution to be homogeneous. Note that ballistic transport can be treated in terms of diffusion due to the randomization of the hot electron momentum through *e-e* and *e-p* collisions and easily incorporated in the theory using the procedure described by Gusev and Wright.[32]

We use the nonstationary Volkov wave functions[33]

$$\Psi_{\mathbf{k}}(\mathbf{r},t)=\Omega^{-1/2}\exp\left[i\left(\mathbf{k}\cdot\mathbf{r}-\int_{-\infty}^{t}\frac{[\hbar\mathbf{k}-e\mathbf{A}(t')/c]^2}{2m\hbar}dt'\right)\right] \tag{1}$$

to represent electronic states of the metal in the presence of the radiation field (here Ω is the crystal volume, and $\mathbf{k}$ is the wave vector of an electron). In principle, this representation of electrons dressed by the field allows exact (nonperturbative) consideration of the field action. Previously, it was successfully applied to a variety of problems such as multiphoton ionization,[34] laser-stimulated electron-atom collisions,[35,36] and high-order harmonic generation.[37]

For the Hamiltonian of interacting electrons and phonons in the presence of the field we write

$$H=H_0+H_{e\text{-}e}+H_{e\text{-}p}, \tag{2}$$

where H_0 is the Hamiltonian for free electrons and phonons in the electromagnetic field,

$$H_0=\sum_{\mathbf{k}}\epsilon_{\mathbf{k}}a_{\mathbf{k}}^{+}a_{\mathbf{k}}+\sum_{j,\mathbf{q}}\hbar\omega_{j,\mathbf{q}}\left(c_{j,\mathbf{q}}^{+}c_{j,\mathbf{q}}+\frac{1}{2}\right), \tag{3}$$

$H_{e\text{-}e}$ represents the electron-electron interaction inside the metal,

$$H_{e\text{-}e}=\sum_{\mathbf{k}_1,\mathbf{k}_2,\mathbf{k}_1',\mathbf{k}_2';\mathbf{K}}W(\mathbf{k}_1',\mathbf{k}_2';\mathbf{p}_1,\mathbf{k}_2;\mathbf{K})a_{\mathbf{k}_1}^{+}a_{\mathbf{k}_2}^{+}a_{\mathbf{k}_1'}a_{\mathbf{k}_2'}, \tag{4}$$

and $H_{e\text{-}p}$ represents electron-phonon interaction inside the metal,

$$H_{e\text{-}p}=\sum_{j,\mathbf{q},\mathbf{k},\mathbf{k}'}M_{\mathbf{k}\to\mathbf{k}'}^{(j,\mathbf{q})}(t)a_{\mathbf{k}'}^{+}a_{\mathbf{k}}(c_{j,-\mathbf{q}}^{+}+c_{j,\mathbf{q}}). \tag{5}$$

The $a_{\mathbf{k}}^{+}(a_{\mathbf{k}})$ are fermion operators of creation (annihilation) of an electron in a quasienergy state with quasimomentum $\mathbf{k}$ and quasienergy $\epsilon_{\mathbf{k}}=\epsilon_{\mathbf{k}}^{0}+\epsilon_{\mathrm{osc}}$, where $\epsilon_{\mathbf{k}}^{0}$ is the electron energy in the absence of the field and $\epsilon_{\mathrm{osc}}=e^2E^2/4m\omega^2$ is the averaged energy of electron oscillations. The $c_{\mathbf{q}}^{+}(c_{\mathbf{q}})$ are boson operators of creation (annihilation) of a phonon with wave vector $\mathbf{q}$ and frequency $\omega_{j,\mathbf{q}}$ belonging to the *j*-phonon branch. We use $W(\mathbf{k}_1',\mathbf{k}_2';\mathbf{k}_1,\mathbf{k}_2;\mathbf{K})$ for the matrix element of the *e-e* transition $\mathbf{k}_1'+\mathbf{k}_2'\to\mathbf{k}_1+\mathbf{k}_2+\mathbf{K}$, where $\mathbf{K}$ is the reciprocal lattice vector. The matrix element of the electron transition from the state $\mathbf{k}$ to the state $\mathbf{k}'$ with emission or absorption of a *j*-branch phonon of wave vector $\mathbf{q}$ is $M_{\mathbf{k}\to\mathbf{k}'}^{(j,\mathbf{q})}$, which is defined by[38]

$$\begin{aligned}M_{\mathbf{k}\to\mathbf{k}'}^{(j,\mathbf{q})}(t)&\equiv\sum_{\mathbf{K}}G_{\mathbf{q},\mathbf{K}}^{(j)}(t)\,\delta_{\mathbf{k}',\mathbf{k}+\mathbf{q}+\mathbf{K}}\\&=\sum_{\mathbf{K}}G_{\mathbf{q},\mathbf{K}}^{(j)}\exp[-i(\mathbf{q}+\mathbf{K})\cdot\boldsymbol{\alpha}(t)]\,\delta_{\mathbf{k}',\mathbf{k}+\mathbf{q}+\mathbf{K}}\\&=\sum_{\mathbf{K}}\left(\frac{\hbar}{2NM\omega_{j,\mathbf{q}}}\right)^{1/2}\\&\quad\times\frac{V'(\mathbf{q}+\mathbf{K})}{\varepsilon(\mathbf{q}+\mathbf{K})}[-i(\mathbf{q}+\mathbf{K})\cdot\mathbf{e}_j(\mathbf{q})]\\&\quad\times\exp[-i(\mathbf{q}+\mathbf{K})\cdot\boldsymbol{\alpha}(t)]\,\delta_{\mathbf{k}',\mathbf{k}+\mathbf{q}+\mathbf{K}},\end{aligned} \tag{6}$$

where N is the number of atoms of the crystal, M is the atomic mass, $\mathbf{e}_j(\mathbf{q})$ is the phonon polarization vector, $\boldsymbol{\alpha}(t)=e\mathbf{E}(t)/m_e\omega^2$ is the electron displacement due to the field. In Eq. (6) $V'(\mathbf{k})$ is the Fourier transform of the ionic pseudopotential $V'(\mathbf{r})$,

$$V'(\mathbf{k})=\Omega_0^{-1}\int V'(\mathbf{r})e^{-i\mathbf{k}\mathbf{r}}d\mathbf{r}, \tag{7}$$

normalized to the volume Ω_0 of the primitive cell of the crystal, and $\varepsilon(\mathbf{q}+\mathbf{K})$ is the dielectric function which accounts for the screening of the pseudopotential by conduction electrons.

The equation for the one-particle electron distribution $f(\mathbf{k},t)=\mathrm{Tr}\{\rho a_{\mathbf{k}}^{+}a_{\mathbf{k}}\}$, where ρ is the statistical operator, can be derived from the Heizenberg equation with the use of the Hamiltonian H (2). For isotropic distributions it reduces to

$$\frac{\partial f(\mathbf{k},t)}{\partial t}=S_{e\text{-}p}+S_{e\text{-}e}, \tag{8}$$

where $S_{e\text{-}p}$ and $S_{e\text{-}e}$ are the e-e and e-p collision integrals, respectively. The e-p collision integral $S_{e\text{-}p}$ is nonlocal in time,

$$\begin{aligned}S_{e\text{-}p}=\hbar^{-2}\sum_{j,\mathbf{q},\mathbf{K}} G^{(j)}_{\mathbf{q},\mathbf{K}}(t)&\\ \times\int_{-\infty}^{t} d\tau G^{(j)}_{-\mathbf{q},-\mathbf{K}}(\tau)[2N_{j,\mathbf{q}}(\tau)+1]&\\ \times\Bigg\{[f(\mathbf{k}+\mathbf{q}+\mathbf{K},\tau)-f(\mathbf{k},\tau)]&\\ \times\exp\left(\frac{i(\epsilon_{\mathbf{k}}-\epsilon_{\mathbf{k}+\mathbf{q}+\mathbf{K}})(\tau-t)}{\hbar}\right)&\\ +[f(\mathbf{k}-\mathbf{q}-\mathbf{K},\tau)-f(\mathbf{k},\tau)]&\\ \times\exp\left(\frac{i(\epsilon_{\mathbf{k}}-\epsilon_{\mathbf{k}-\mathbf{q}-\mathbf{K}})(t-\tau)}{\hbar}\right)\Bigg\},&\end{aligned} \tag{9}$$

where $N_{j,\mathbf{q}}(t)$ is the distribution function of phonons in the j branch. Deriving Eq. (9) we assumed that e-p collisions are quasielastic. This approximation may be justified by the fact that the energy relaxation of the electron gas in metals is determined by electron-electron collisions rather than electron-phonon collisions.

We are interested in calculating the value of the electron distribution averaged over the laser period. We denote the time-averaged $f(\mathbf{k},t)$ by $\overline{f}(\mathbf{k},t)$, and similarly for other quantities. If $\omega\tau_{e\text{-}e}\gg 1$ and $\omega\tau_{e\text{-}p}\gg 1$ (here $\tau_{e\text{-}e}^{-1}$ and $\tau_{e\text{-}p}^{-1}$ are the characteristic e-e and e-p collision rates, respectively) the mean integral of e-p collision can be reduced to the form

$$\begin{aligned}\overline{S}_{e\text{-}p}=\frac{2\pi}{\hbar}\sum_{n}\sum_{j,\mathbf{q},\mathbf{K}}|G^{(j)}_{\mathbf{q},\mathbf{K}}|^2(2\overline{N}_{j,\mathbf{q}}+1)J_n^2\left(\frac{e\mathbf{E}_0(t)\cdot(\mathbf{q}+\mathbf{K})}{m\omega^2}\right)&\\ \times[\overline{f}(\mathbf{k}+\mathbf{q}+\mathbf{K},t)-\overline{f}(\mathbf{k},t)]\delta(\epsilon_{\mathbf{k}}+n\hbar\omega-\epsilon_{\mathbf{k}+\mathbf{q}+\mathbf{K}}),&\end{aligned} \tag{10}$$

where $J_n(x)$ is a Bessel function of order n. The e-p collision integral (10) includes contributions of all possible laser-stimulated normal and umklapp processes with participation of acoustic phonons.

The phonon distribution $\overline{N}_{j,\mathbf{q}}(t)$ satisfies a kinetic equation similar to Eq. (8) and may be nonequilibrium in the time domain of interest. Nevertheless, here we will neglect its time dependence and use the equilibrium

$$\overline{N}_{j,\mathbf{q}}(t)=\{\exp[\hbar\Omega_{j\cdot\mathbf{q}}/kT_l(t)]-1\}^{-1}, \tag{11}$$

where T_l is the temperature of the lattice.

The e-e collision integral we approximate with the form

$$\overline{S}_{e\text{-}e}=\frac{f_0(\epsilon_{\mathbf{k}},T_e(t))-\overline{f}(\mathbf{k},t)}{\tau_{e\text{-}e}(\mathbf{k})}, \tag{12}$$

where $\tau_{e\text{-}e}(\mathbf{k})$ is the e-e relaxation time, $f_0(\epsilon_{\mathbf{k}},T_e(t))=\{\exp[(\epsilon_{\mathbf{k}}-\epsilon_F)/kT_e(t)]+1\}^{-1}$ is the equilibrium distribution. We define the effective electron temperature $T_e(t)$ in Eq. (12) by the relation

$$W(t)=W_0+\frac{\gamma T_e^2(t)}{2}=\frac{1}{4\pi^3}\int\epsilon_{\mathbf{k}}\overline{f}(\mathbf{k},t)d\mathbf{k}, \tag{13}$$

where $W(t)$ is the energy density of the electron gas averaged over laser period, $W_0=3n\epsilon_F/5$ is the energy density of the Fermi electron gas in the ground state ($T_e=0$ K), $\gamma=\pi^2nk_B^2/2\epsilon_F$, and n is the electron density. This definition of the temperature T_e reflects the fact that electron collisions result in the energy redistribution among the electrons without changing their total energy.

III. COLLISION RATES

Before proceeding to analysis of Eq. (8) we consider the energy dependence of the e-e and e-p collision rates $\tau_{e\text{-}e}^{-1}$ and $\tau_{e\text{-}p}^{-1}$, which to a large extent determine the ultrafast relaxation dynamics.

A. Electron-electron collisions

The e-e scattering rate in noble metals is currently a matter of intensive discussion. This is connected with the recent findings of quantitative and qualitative disagreement between the experimental rates and the predictions given by the Fermi-liquid theory.[17–19] This deviation manifests itself when the laser can excite d-band electrons of the noble metal.[18] Much better agreement between the experimental and theoretical rates is observed when no transitions from the d bands to sp band are possible.[19,39] In our case this condition is well fulfilled since the laser frequency is sufficiently small. For the e-e collisions rate $1/\tau_{e\text{-}e}$ we write[38]

$$\begin{aligned}\tau_{e\text{-}e}^{-1}(\mathbf{k}_1)=\frac{8\pi^4}{\hbar\Omega}\sum_{\mathbf{k}_2,\mathbf{k}_1',\mathbf{k}_2'}|g(\mathbf{k}_1,\mathbf{k}_2,\mathbf{k}_1',\mathbf{k}_2')|^2&\\ \times\delta(\mathbf{k}_1+\mathbf{k}_2-\mathbf{k}_1'-\mathbf{k}_2')f(\mathbf{k}_2)[1-f(\mathbf{k}_1')]&\\ \times[1-f(\mathbf{k}_2')]\delta(\epsilon_{\mathbf{k}_1}+\epsilon_{\mathbf{k}_2}-\epsilon_{\mathbf{k}_1'}-\epsilon_{\mathbf{k}_2'}),&\end{aligned} \tag{14}$$

where Ω is the volume of the crystal, $f(\mathbf{k})$ is the distribution function of electrons, and $|g(\mathbf{k}_1,\mathbf{k}_2,\mathbf{k}_1',\mathbf{k}_2')|^2$ is the square of the transition matrix element summed over spin coordinates given by

$$\begin{aligned}|g(\mathbf{k}_1,\mathbf{k}_2,\mathbf{k}_1',\mathbf{k}_2')|^2=2[V_{ee}^2(\mathbf{k}_1'-\mathbf{k}_1)+V_{ee}^2(\mathbf{k}_1'-\mathbf{k}_2)&\\ -V_{ee}(\mathbf{k}_1'-\mathbf{k}_1)V_{ee}(\mathbf{k}_1'-\mathbf{k}_2)],&\end{aligned} \tag{15}$$

where $V_{ee}(\mathbf{k})$ is the Fourier transform of the screened Coulomb potential

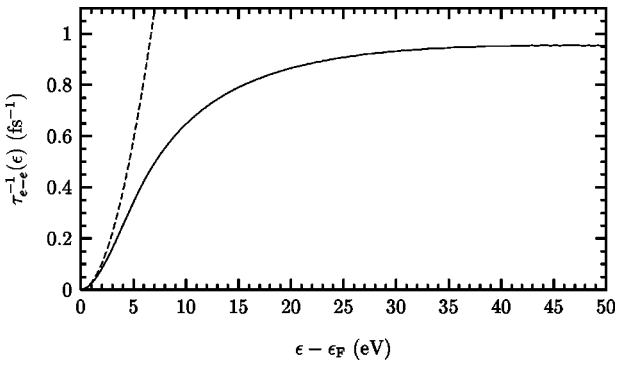

FIG. 1. The e-e scattering rate $\tau_{e\text{-}e}^{-1}$ in gold versus hot-electron energy ϵ. The solid line corresponds to the scattering rate calculated with the use of Monte Carlo integration of Eq. (18) and the dashed lines correspond to e-e scattering rates calculated by formula (19). The Fermi energy is denoted by ϵ_F. The electron temperature T_e is 350 K.

$$V_{ee}(\mathbf{k}) = \frac{e^2}{\Omega \varepsilon_0} \cdot \frac{1}{k^2 + q_s^2}. \tag{16}$$

The first term on the right-hand side of Eq. (15) accounts for the direct e-e interaction, while the second and third terms are responsible for the exchange interaction. The value q_s in Eq. (16) is the screening wave number which, in the Thomas-Fermi treatment, is

$$q_s = \sqrt{3ne^2/2\varepsilon_0 \epsilon_F}, \tag{17}$$

where n is the conduction electron density and ε_0 is the dielectric constant.

We calculated the scattering rate $1/\tau_{e\text{-}e}$ using Eq. (14) with the use of Monte Carlo integration. To do this we transform Eq. (14) to

$$\begin{aligned}\tau_{e\text{-}e}^{-1}(\mathbf{k}_1) = {} & \frac{e^4}{8(2\pi)^5 \hbar \varepsilon_0^2} \int d\mathbf{k}_2 d\Omega_{\mathbf{q}} q \\ & \times \left(\frac{1}{[(\mathbf{k}_1' - \mathbf{k}_1)^2 + q_s^2]^2} + \frac{1}{[(\mathbf{k}_1' - \mathbf{k}_2)^2 + q_s^2]^2} \right. \\ & \left. - \frac{1}{[(\mathbf{k}_1' - \mathbf{k}_1)^2 + q_s^2][(\mathbf{k}_1' - \mathbf{k}_2)^2 + q_s^2]} \right) \\ & \times f(\mathbf{k}_2)[1 - f(\mathbf{k}_1')][1 - f(\mathbf{k}_2')]\end{aligned} \tag{18}$$

with accounting of Eqs. (15) and (16) and using the equality

$$\begin{aligned}\delta(\mathbf{k}_1 + \mathbf{k}_2 - \mathbf{k}_1' - \mathbf{k}_2') = 8^{-1} \int & \delta\left(\mathbf{k}_1' - \frac{1}{2}(\mathbf{k}_1 + \mathbf{k}_2 + \mathbf{q}) \right) \\ & \times \delta\left(\mathbf{k}_2' - \frac{1}{2}(\mathbf{k}_1 + \mathbf{k}_2 - \mathbf{q}) \right) d\mathbf{q}.\end{aligned}$$

In Eq. (18) $d\Omega_{\mathbf{q}} = \sin\theta_{\mathbf{q}} d\theta_{\mathbf{q}} d\varphi_{\mathbf{q}}$, $\theta_{\mathbf{q}}$ and $\varphi_{\mathbf{q}}$ are the tangential and polar angles of the vector $\mathbf{q}$ of length $q = |\mathbf{k}_1 - \mathbf{k}_2|$, $\mathbf{k}_1' = \frac{1}{2}(\mathbf{k}_1 + \mathbf{k}_2 + \mathbf{q})$ and $\mathbf{k}_2' = \frac{1}{2}(\mathbf{k}_1 + \mathbf{k}_2 - \mathbf{q})$.

Figure 1 shows the dependence of the e-e scattering rate in gold on the hot-electron energy $\epsilon_{\mathbf{k}} - \epsilon_F$. Here we take $f(\mathbf{k})$ to be the Fermi distribution at the electron temperature $T_e = 350$ K. The solid line corresponds to the rate calculated by Eq. (18). Also shown in Fig. 1, as dashed line, the e-e scattering rates obtained with the often-used formula[38,40]

$$\tau_{e\text{-}e}^{-1}(k) = \frac{e^4 (k_B T_e)^2}{16\pi\hbar^4 \varepsilon_0^2 v^3 k} \cdot \left[1 + \left(\frac{\epsilon_{\mathbf{k}} - \epsilon_F}{\pi k_B T_e} \right)^2 \right] \cdot \gamma(2k/q_s), \tag{19}$$

where v is the electron velocity ($v = \hbar k/m$), and

$$\gamma(x) = \frac{x^3}{4} \left(\arctan x + \frac{x}{1 + x^2} - \frac{\arctan(x\sqrt{x^2+2})}{\sqrt{x^2+2}} \right), \tag{20}$$

which is valid for $\epsilon_{\mathbf{k}} - \epsilon_F \ll \epsilon_F$.

The behavior of the e-e scattering rate is mainly determined by two factors. The first factor is Pauli's exclusion principle which is responsible for the $(\epsilon_{\mathbf{k}} - \epsilon_F)^2$ increase in the e-e scattering rate when $0 < \epsilon_{\mathbf{k}} - \epsilon_F < \epsilon_F$. Outside of this region, the e-e scattering rate tends to the e-e scattering rate in plasma which falls as $\epsilon_{\mathbf{k}}^{-3/2}$ due to the decay in the e-e cross-section with increasing relative electron velocity. In Fig. 1 we see how the e-e scattering rate calculated by formula (18) saturates to its maximum value which does not exceed 1 fs^{-1}, thereby improving on the range of validity of Eq. (19). The energy range where the e-e scattering rate decays is not shown in Fig. 1 as it is outside of the domain of interest.

To avoid expensive calculations, in what follows, we employ the relaxation rate calculated by Eq. (18) assuming that $f(\mathbf{k})$ is the equilibrium distribution. This is due to the fact that the difference between the relaxation rates calculated with or without accounting of the nonequilibrium part of the electron distribution is not significant for hot electrons.[41]

B. Electron-phonon collisions

As follows from Eq. (10) the rate of e-p collisions with simultaneous absorption or emission of n photons is[41]

$$\begin{aligned}\frac{1}{\tau_{e\text{-}p}^{(n)}(\mathbf{k})} = {} & \frac{2\pi}{\hbar} \sum_{j,\mathbf{q},\mathbf{K}} |G_{\mathbf{q},\mathbf{K}}^{(j)}|^2 [2N(\omega_{j,\mathbf{q}}) + 1] \\ & \times J_n^2 \left(\frac{e\mathbf{E}_0 \cdot (\mathbf{q} + \mathbf{K})}{m\omega^2} \right) \delta(\epsilon_{\mathbf{k}} + n\hbar\omega - \epsilon_{\mathbf{k}+\mathbf{q}+\mathbf{K}}),\end{aligned} \tag{21}$$

where $\mathbf{k}$ is the electron wave vector. To calculate the e-p collision rate $1/\tau_{e\text{-}p}^{(n)}$ we will apply the Debye model which prescribes the same dispersion relations for different j branches

$$\omega_{j,\mathbf{q}} = \omega_{\mathbf{q}} = sq \tag{22}$$

and restricts the possible phonon states with wave vector $\mathbf{q}$ to the sphere of radius $q_D = (2/Z)^{1/3} k_F$, where Z is the number of conduction electrons per ion.[42] Here s is the speed of sound in the metal. The expression for $1/\tau_{e\text{-}p}^{(n)}$ may be simplified by elementary summing over j in Eq. (21), and with the use of Eq. (6) can be reduced to

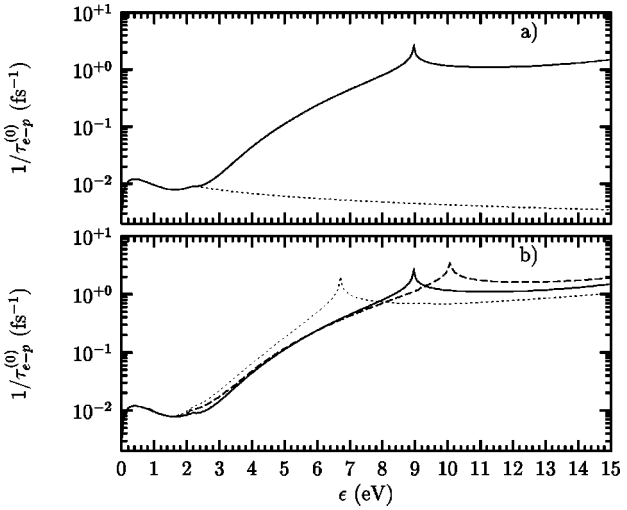

FIG. 2. (a) The energy dependencies of the e-p collision rate $1/\tau^{(0)}_{e\text{-}p}$ calculated by formula (23) with (solid line) and without (dotted line) accounting of umklapp processes for the orientation of the electron wave vector $\hat{\mathbf{k}}=\hat{\mathbf{z}}$. (b) The rate, with umklapp processes, for three different directions of the electron wave vector, solid line $\hat{\mathbf{k}}=\hat{\mathbf{z}}$, dashed line $\hat{\mathbf{k}}=(\hat{\mathbf{x}}+\hat{\mathbf{z}})/\sqrt{2}$, and dotted line $\hat{\mathbf{k}}=(\hat{\mathbf{x}}+\hat{\mathbf{y}}+\hat{\mathbf{z}})/\sqrt{3}$.

$$\frac{1}{\tau^{(n)}_{e\text{-}p}(\mathbf{k})}=\frac{1}{8\pi^2\rho}\sum_{\mathbf{K}}\int d\mathbf{q}\frac{(\mathbf{q}+\mathbf{K})^2}{\omega_{\mathbf{q}}}\left(\frac{V'(\mathbf{q}+\mathbf{K})}{\varepsilon(\mathbf{q}+\mathbf{K})}\right)^2 \times[2N(\hbar\omega_{\mathbf{q}})+1]J_n^2\left(\frac{e\mathbf{E}_0\cdot(\mathbf{q}+\mathbf{K})}{m\omega^2}\right) \times\delta(\epsilon_{\mathbf{k}}+n\hbar\omega-\epsilon_{\mathbf{k}+\mathbf{q}+\mathbf{K}}), \tag{23}$$

where ρ is the density of the metal. For the Fourier transform of the ion pseudopotential $V'(\mathbf{k})$ we use the Harrison form

$$V'(\mathbf{k})=\frac{e^2}{4\pi\epsilon_0\Omega_0}\left(-\frac{4\pi Z}{k^2}+\frac{\beta}{(1+k^2r_c^2)^2}\right), \tag{24}$$

where the parameters β and r_c are taken from Ref. 43. For the dielectric function $\varepsilon(\mathbf{k})$ in Eq. (23) we use the Lindhard's form.[42] Then, one integration in Eq. (23) can be performed with the use of the δ function and the substitution $\mathbf{k}'=\mathbf{k}+\mathbf{q}+\mathbf{K}$. The resultant two-dimensional integral has been calculated numerically. The summation in Eq. (23) has been carried out over those vectors $\mathbf{K}$ for which the phonon states lie within the Debye sphere.

The e-p collision rate $1/\tau^{(0)}_{e\text{-}p}$ calculated for gold by using Eq. (23) is presented in Fig. 2(a). The solid line was calculated with accounting of umklapp processes while the dotted line was calculated with them being ignored. The steady decay of the dashed line is connected with the cutoff of the phonon spectrum at $q=q_D$. Taking into account that the maximum change in the electron wave vector $2k$ cannot exceed q_D one can see that the cutoff restricts the phase space of the electron final states when $\epsilon_{\mathbf{k}}>\hbar^2q_D^2/4m$ (in our case $\hbar^2q_D^2/4m=2.7$ eV). Figure 2(b) shows the same dependencies calculated for three different directions of the electron wave vectors $\hat{\mathbf{k}}$, namely, $\hat{\mathbf{k}}=\mathbf{k}/k=\hat{\mathbf{z}}$ for solid line, $\hat{\mathbf{k}}=(\hat{\mathbf{x}}+\hat{\mathbf{z}})/\sqrt{2}$ for dashed line and $\hat{\mathbf{k}}=(\hat{\mathbf{x}}+\hat{\mathbf{y}}+\hat{\mathbf{z}})/\sqrt{3}$ for dotted line. Note that in the chosen orthogonal basis determined by vectors $\hat{\mathbf{x}}$, $\hat{\mathbf{y}}$, and $\hat{\mathbf{z}}$ the primitive vectors of the reciprocal lattice are $\mathbf{b}_1=2\pi(\hat{\mathbf{y}}+\hat{\mathbf{z}}-\hat{\mathbf{x}})/a$, $\mathbf{b}_2=2\pi(\hat{\mathbf{x}}+\hat{\mathbf{z}}-\hat{\mathbf{y}})/a$, and $\mathbf{b}_3=2\pi(\hat{\mathbf{x}}+\hat{\mathbf{y}}-\hat{\mathbf{z}})/a$.

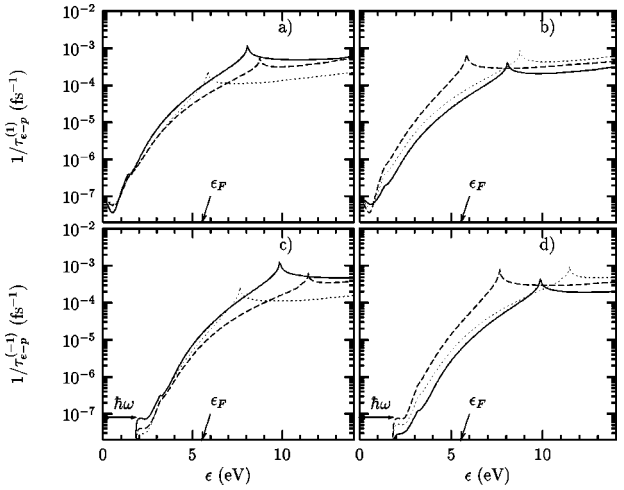

FIG. 3. Electron-phonon collision rates (a) and (b) $1/\tau^{(1)}_{e\text{-}p}$ and (c) and (d) $1/\tau^{(-1)}_{e\text{-}p}$ versus electron energy. The solid, dashed, and dotted lines correspond to the rates calculated for three different directions of the electron wave vector $\hat{\mathbf{k}}=\hat{\mathbf{z}}$, $\hat{\mathbf{k}}=(\hat{\mathbf{x}}+\hat{\mathbf{z}})/\sqrt{2}$, and $\hat{\mathbf{k}}=(\hat{\mathbf{x}}+\hat{\mathbf{y}}+\hat{\mathbf{z}})/\sqrt{3}$, respectively. The orientation of the electric field of the wave are chosen to be (a) and (c) $\hat{\mathbf{z}}$ and (b) and (d) $(\hat{\mathbf{x}}+\hat{\mathbf{y}}+\hat{\mathbf{z}})/\sqrt{3}$.

Figure 2 reveals the anisotropy and the resonant structure of the e-p collision rate. The resonant structure of the e-p collision rate is associated with electron scattering on Bragg planes. In our calculations we used one-plane-wave model which is not applicable in the vicinity of Bragg planes.[38] However, the characteristic size of these regions is very small $\sim 0.04\times 2\pi/a$ in comparison with the characteristic scale of an electron wave vector $k_F\sim 2\pi/a$, where a is a length of a side of a conventional cubic cell.[38] Figure 2 also reveals dramatic difference between the normal and umklapp components of the e-p collision rate when $\epsilon_{\mathbf{k}}>\hbar^2q_D^2/4m$. This difference results from the fact that the phase space of the possible final electron states diminishes for normal processes and rises for umklapp collisions with increasing energy.

The rates of e-p collisions in gold accompanied by emission or absorption of one photon for two different orientations of the electric field vector $\mathbf{E}_0$ of the wave are shown in Fig. 3. As in Fig. 2, these rates were calculated for three different directions of the electron wave vector $\mathbf{k}$. The orientation of the vector $\mathbf{E}_0$ is $\mathbf{z}$ for Figs. 3(a) and 3(c) and $(\hat{\mathbf{x}}+\hat{\mathbf{y}}+\hat{\mathbf{z}})/\sqrt{3}$ for Figs. 3(b) and 3(d). Since the electric field of the wave $\mathbf{E}_0$ appears in combination $(\mathbf{E}_0\cdot\mathbf{q}+\mathbf{K})/m\omega^2$ [see Eq. (21)], we characterize the field magnitude by the multiphoton parameter $X=eE_0k_F/m\omega^2$. In the low-field limit ($X\ll 1$) this parameter is equal to the number of photons absorbed in an e-p collision event.[44] In these calculations we used $X=0.019$ and $\hbar\omega=1.84$ eV.

Figure 3 demonstrates the same features we discussed considering the e-p collision rate without absorption or emission of photons. These features are the anisotropy and

the resonant structure of the collision rates and also domination of the umklapp collisions over the normal collisions when electron energies are higher than the Fermi energy. In addition, we see that the laser stimulated e-p collision rates depend on the orientation of the electric strength vector with respect to the crystal axis.

IV. NUMERICAL SOLUTION OF THE KINETIC EQUATION

In this section we look for the solution of Eq. (8) with e-p and e-e collision integrals determined respectively by relations (10) and (12). To compare with the experiment[12] we are particularly interested in the behavior of this solution in the energy region from ϵ_F to $\epsilon_F+\hbar\omega$. Also, we consider here only the low-field ($X\ll 1$) limit which applies to the experimental conditions.

In the limit $X\ll 1$ production of electrons in the region of interest is mainly determined by the one-photon indirect transitions. The contributions of multiphoton and cascade processes are of higher order in the multiphoton parameter X, and can be neglected. Here we determine a multiphoton transition as a transition from the initial state $\epsilon_{\mathbf{k}_i}$ to the final state $\epsilon_{\mathbf{k}_f}=\epsilon_{\mathbf{k}_i}+n\hbar\omega$ with absorption (or emission) of some integer n ($|n|>1$) of photons in a single e-p collision. A multiphoton transition is not a unique way for an electron to come to the final state $\epsilon_{\mathbf{k}_f}$ from the initial state $\epsilon_{\mathbf{k}_i}$. Any other transition from $\epsilon_{\mathbf{k}_i}$ to $\epsilon_{\mathbf{k}_f}$ with two or more successive e-p collisions we call a cascade transition. We also specify a one-photon cascade where each e-p collision is accompanied by only one-photon emission (or absorption).

Outside the region $\epsilon_F<\epsilon_{\mathbf{k}}<\epsilon_F+\hbar\omega$, the electron distribution can depend on both multiphoton and cascade processes. Comparing their contributions to the distribution function one can see that the relative weight of these processes is determined by the ratio of the e-e and e-p collision rates $1/\tau_{e\text{-}e}$ and $1/\tau^{(0)}_{e\text{-}p}$.[27] It follows from the following estimations for the contribution of n-photon transitions,

$$\delta f_n \sim \frac{\tau_{e\text{-}e}(\epsilon)}{\tau^{(n)}_{e\text{-}p}(\epsilon)}, \tag{25}$$

and the corresponding contribution of one-photon cascade processes that

$$\delta f_1 \sim \prod_{k=0}^{n-1} \frac{\tau_{e\text{-}e}(\epsilon-k\hbar\omega)}{\tau^{(1)}_{e\text{-}p}(\epsilon-k\hbar\omega)}, \tag{26}$$

and the estimate $1/\tau^{(n)}_{e\text{-}p}(\epsilon)\approx J_n^2(X)/\tau^{(0)}_{e\text{-}p}(\epsilon-\hbar\omega)$.[27] The expressions on the right-hand side of Eqs. (25) and (26) are nothing more than the probability of the corresponding processes. Thus when $1/\tau_{e\text{-}e}\ll 1/\tau^{(0)}_{e\text{-}p}$ one-photon cascade processes dominate, and conversely the distribution is governed by multiphoton processes if $1/\tau_{e\text{-}e}\gg 1/\tau^{(0)}_{e\text{-}p}$. Both multiphoton and cascade mechanisms give rise to a similar structure of the distribution function. The difference between these two limiting cases is in the fact that the electron distribution is isotropic when $1/\tau_{e\text{-}e}\ll 1/\tau^{(0)}_{e\text{-}p}$ and anisotropic when $1/\tau_{e\text{-}e}\gg 1/\tau^{(0)}_{e\text{-}p}$.[27]

Figure 4 depicts the e-e and e-p collision rates $1/\tau_{e\text{-}e}$ and $1/\tau^{(0)}_{e\text{-}p}$ versus energy which were found by numerical integration of Eqs. (18) and (23), respectively. One can see that the e-p collision rate $1/\tau^{(0)}_{e\text{-}p}$ is significantly larger than the e-e scattering rate $1/\tau_{e\text{-}e}$ for all considered $\epsilon_{\mathbf{k}}$. Thus here we deal with the case where the distribution is mainly determined by one-photon cascade processes. That allows us to simplify the problem by neglecting all multiphoton terms in the e-p collision integral (10), and assuming that the electron distribution is isotropic. Then the equation governing the electron distribution (8) is reduced to

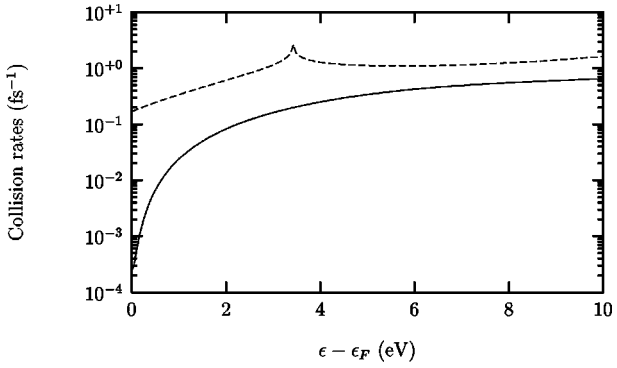

FIG. 4. Electron-electron (solid line) and electron-phonon (dashed line) collision rates $1/\tau_{e\text{-}e}$ and $1/\tau^{(0)}_{e\text{-}p}$ versus hot-electron energy ϵ.

$$\frac{\partial\overline{f}(\epsilon_{\mathbf{k}},t)}{\partial t}=\frac{f_0(\epsilon_{\mathbf{k}},T_e(t))-\overline{f}(\epsilon_{\mathbf{k}},t)}{\tau_{e\text{-}e}(\epsilon_{\mathbf{k}})}+S^{(1)}_{e\text{-}p}(\epsilon_{\mathbf{k}},t)+S^{(-1)}_{e\text{-}p}(\epsilon_{\mathbf{k}},t), \tag{27}$$

where now

$$S^{(\pm1)}_{e\text{-}p}(\epsilon_{\mathbf{k}},t)=\frac{\overline{f}(\epsilon_{\mathbf{k}}\pm\hbar\omega,T_e(t))-\overline{f}(\epsilon_{\mathbf{k}},T_e(t))}{\tau^{(\pm1)}_{e\text{-}p}(\epsilon_{\mathbf{k}})} \tag{28}$$

and

$$\frac{1}{\tau^{(\pm1)}_{e\text{-}p}(\epsilon_{\mathbf{k}})}=\frac{1}{4\pi}\int\frac{1}{\tau^{(\pm1)}_{e\text{-}p}(\mathbf{k})}d\Omega. \tag{29}$$

The distribution $\overline{f}(\epsilon_{\mathbf{k}},t)$ satisfies the initial condition

$$\overline{f}(\epsilon_{\mathbf{k}},t_0)=f_0(\epsilon_{\mathbf{k}},T_e(t_0)), \tag{30}$$

where t_0 corresponds to the beginning of the laser pulse and $T_e(t_0)$ is the initial electron temperature.

To find the distribution function $\overline{f}(\epsilon_{\mathbf{k}})$ from Eq. (27), with the initial condition (30), we need the time-dependent electron temperature $T_e(t)$ which is a functional of the distribution function (13). However, we cannot use directly relation (13) together with Eq. (27) in our calculations. The reason is that the quasielastic approximation which we used to derive the expression for the e-p collision integral (9) does not allow consideration of energy transfer from the electrons to the lattice.

To account for this process we transform Eq. (13) with the use of Eq. (27) to the differential form

$$C_e(T_e)\frac{dT_e}{dt}=\sum_n \frac{1}{4\pi^3}\int \epsilon_{\mathbf{k}} S^{(n)}_{e\text{-}p} d\mathbf{k}, \tag{31}$$

where $C_e(T_e)=\gamma T_e$ is the specific-heat capacity of the electron gas. Deriving Eq. (31) we took into account that e-e collisions do not change the total energy of the electron gas.

The zeroth term of the expansion on the right-hand side of Eq. (31) is the electron-lattice energy transfer rate. In the quasielastic approximation this term drops out. Here, however, we use the relation for the energy transfer rate derived by Allen:[45]

$$\frac{1}{4\pi^3}\int \epsilon_{\mathbf{k}} S^{(0)}_{e\text{-}p} d\mathbf{k}=g(T_l-T_e), \tag{32}$$

where T_l is the lattice temperature. In Eq. (32) the thermal relaxation rate g is

$$g=\frac{3\hbar\,\gamma\overline{\lambda}\langle\Omega^2\rangle}{\pi k_B^2}, \tag{33}$$

$\overline{\lambda}$ is the e-p coupling constant and $\langle\Omega^2\rangle$ is the second moment of the phonon spectrum defined by McMillan.[46]

The remaining terms of the expansion (31) compose the total rate of laser energy absorption by the electrons

$$S(t)=\sum_{n\neq 0}\frac{1}{4\pi^3}\int \epsilon_{\mathbf{k}} S^{(n)}_{e\text{-}p} d\mathbf{k}. \tag{34}$$

We will treat these terms in the quasielastic approximation. In the low-field limit only linear terms of the laser intensity can survive in the expansion of the right-hand side of Eq. (34). So, one can see that the source term depends functionally on the laser intensity as

$$S(t)=\mu I(t), \tag{35}$$

where coefficient μ characterizes the absorptivity of the metal.

Finally, we have the following differential equation for the electron temperature T_e:

$$C_e(T_e)\frac{dT_e}{dt}=-g(T_e-T_l)+S(t) \tag{36}$$

which, together with the equation for the lattice temperature T_l,

$$C_l\frac{dT_l}{dt}=g(T_e-T_l), \tag{37}$$

forms the set of equations of the two-temperature model. In Eq. (37) the constant C_l is the lattice specific-heat capacity.

Here we report the results of the numerical solution of the set of Eqs. (27) and (36). The absorbed laser intensity $I(t)$ was assumed to be of the Gaussian form $I(t)=I_0\exp[-t^2/\tau_L^2]$, where I_0 is the maximum value of the intensity and τ_L is the laser pulse duration. When calculating the electron temperature T_e we assumed that the lattice temperature T_l is constant ($T_l=300$ K). The optical source term $S(t)$ was calculated by using Eq. (34). We used the laser radiation parameters similar to those of the experiment:[12] the

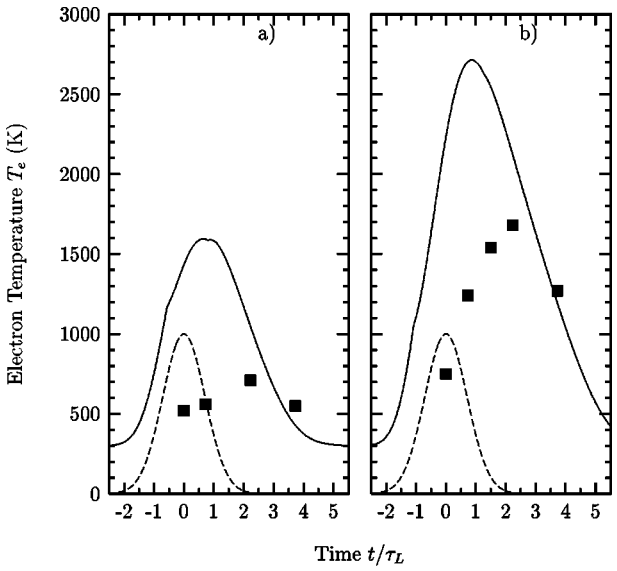

FIG. 5. Time dependence of the electron temperature T_e calculated at the absorbed laser intensity (a) $I_0=0.67\times10^9$ W cm^{-2} and (b) $I_0=1.67\times10^9$ W cm^{-2}. The points correspond to the temperatures T_e' estimated by Fann *et al.*[12] (see text). Also shown, by the dashed line, is the laser pulse Gaussian envelope (arbitrary units). The pulse duration is denoted by $\tau_L=180$ fs.

absorbed laser intensity $I_0=(0.67\pm0.22)\times10^9$ W cm^{-2} or $I_0=(1.67\pm0.5)\times10^9$ W cm^{-2}, the photon energy $\hbar\omega=1.84$ eV, and the laser pulse duration $\tau_L=180$ fs. For the gold target we used: the Fermi energy $\epsilon_F=5.53$ eV, the thermal relaxation rate $g=2.7\times10^{17}$ W m^{-1} K^{-1},[47] and the coefficient in the electron specific-heat capacity $\gamma=62.64$ J m^{-3} K^{-2}.

Note that Fann *et al.*,[11] in trying to explain their measurements, used a different value for the thermal relaxation rate g, namely $g=4\times10^{16}$ W m^{-1} K^{-1}.[11,12] This is an order of magnitude lower than the value arising from Allen's formula (33). To determine their value, Fann *et al.* first found the electron temperature T_e' for different instants of time by fitting the experimental distributions with the Fermi-Dirac distribution. Then the thermal relaxation rate g is extracted by fitting T_e' with the solution of the two-temperature model equations. However, the temperature T_e' can be used as a measure of the energy of the electron system provided that the distortion $\delta f(\epsilon_{\mathbf{k}})$ of the electron distribution is small compared with the equilibrium distribution $f_0(\epsilon_{\mathbf{k}},T_e')$. The experiment[12] shows that this is not the case. The significant amount of the absorbed energy is stored in the ''nonequilibrium'' electrons during the irradiation. That means that in the considered case the two-temperature model is not applicable for the description of the time behavior of the temperature T_e'. We saw that a straightforward generalization of the two-temperature model to the ultrashort laser pulse case can be provided by a different definition (13) of the electron temperature.

This situation is illustrated in Fig. 5. It shows the time dependence of the electron temperature T_e calculated with the use of Eq. (36). The solid squares represent the electron temperatures T_e' estimated from the experimental data by Fann *et al.*[12] We see that the electron temperature T_e is several times larger than T_e' during the laser action. This is due

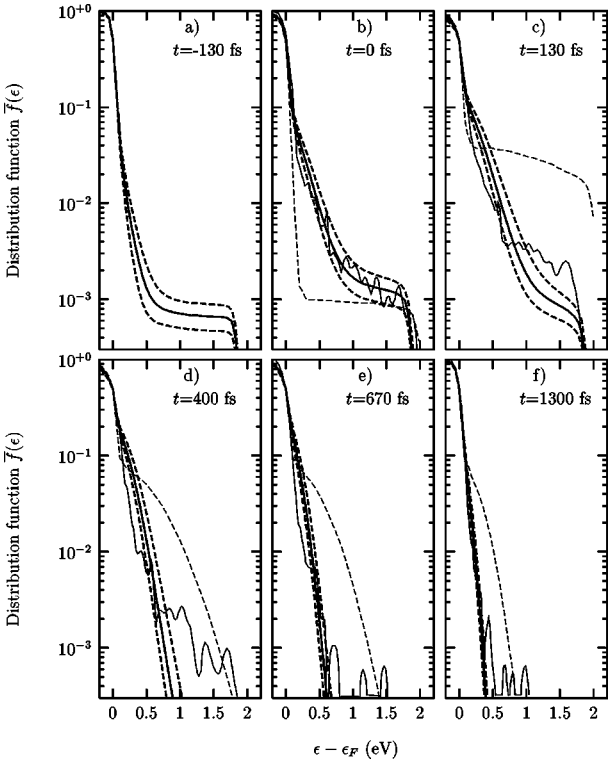

FIG. 6. Electron distribution function $\bar{f}(\epsilon_{\mathbf{k}})$ versus energy at different time instants. The thick solid and dashed (see text) lines represent our calculations, the thin solid lines are the experimental distributions[12] and the thin dashed lines are the calculations of Bejan and Raşeev.[31] The mean absorbed laser intensity is 0.67×10^9 W cm^{-2}.

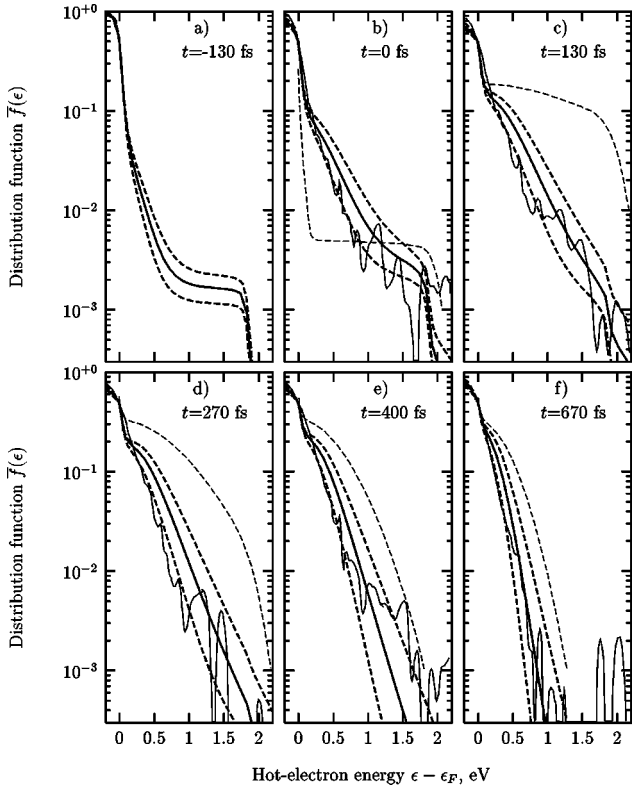

FIG. 7. Same as for Fig. 6 except for laser absorbed intensity of 1.67×10^9 W.

to the fact that a substantial portion of the absorbed energy is in the nonequilibrium part of the distribution. We see that the temperature T_e reaches its maximum at $t \approx \tau_L$. At this moment the energy absorption rate from the laser field is equal to the rate of energy transfer from the electrons to the lattice. The two methods for evaluating the temperature of the electrons become in good agreement once the electrons have had sufficient time to return to the equilibrium. This occurs for $t > 2\tau_L$.

In Fig. 6 we show the calculated electron distributions (thick solid lines) produced in gold at $I_0 = 0.67 \times 10^9$ W cm^{-2} ($X = 0.019$). The thick dashed lines indicate the distributions calculated at the absorbed laser intensity $I_0 = (0.67 \pm 0.22) \times 10^9$ W cm^{-2} to see the effect of the experimental uncertainty in I_0 on the results. The thin solid lines are the experimentally found distributions.[12] Agreement with experiment is found whenever the thin solid line is within the two thick dashed lines. For comparison, we also give the distributions calculated by Bejan and Raşeev[31] as thin dashed lines. Unfortunately, the numerical calculations of the distribution function presented in Ref. 30 were conducted for a different set of laser parameters and do not allow for comparison here.

In the experiment the pulse duration is 180 fs with the individual parts of Fig. 6 showing snapshots of the electron distribution functions. The case $t = 0$ fs [Fig. 6(b)] corresponds to the case when the pulse maximum is incident on the surface, and is when the measurements begin. We see generally very good agreement with experiment, which is much better than with the calculation of Bejan and Raşeev.[31] Figure 6(a) shows an almost flat energy distribution in the region from 0.5–1.84 eV at the moment $t = -130$ fs. The next picture [Fig. 6(b)] demonstrates that this flat distribution is significantly deformed at the maximum of the laser pulse. This deformation is due to the *e-e* collisions. Note the excellent agreement between the experimental data and our calculations in this particular case. This agreement is not as good for the following time instants [Figs. 6(c) and 6(d)]. The calculations show that the deviation in the absorbed laser intensity I_0 cannot explain the significant number or distribution structure of hot electrons between 1 and 1.84 eV. With increasing t our results converge to the Fermi distribution as expected, unlike the calculations of Bejan and Raşeev.[31]

Figure 7 presents similar experimental and theoretical dependencies for the electron distributions produced by the laser pulse at the laser absorbed intensity $I_0 = (1.67 \pm 0.5) \times 10^9$ W cm^{-2}. Comparison of our calculations with the experiment[12] also shows generally good agreement. The best fit for the experiment is provided by the distributions calculated at the lowest value of the intensity $I_0 = 1.17 \times 10^9$ W cm^{-2}. However, this distribution gives a lower number of hot electrons above 1 eV than that observed in the experiment. As in the previous figure the present calculations give a much better account of the experimental data than the calculations of Bejan and Raşeev.[31] We suspect that this is because the mechanism suggested by Bejan and Raşeev for production of hot electrons in metals is incorrect. They assume that this process is due to direct resonant dipole transitions between two levels in the conduction band. However,

in the dipole approximation such transitions cannot take place. This follows from the energy and quasimomentum conservation.[42,48]

V. CONCLUSIONS

In this work we considered the problem of the electron distribution evolving in a metal during ultrashort laser pulse action. We have shown that interplay between electron-electron scattering and laser-stimulated electron phonon collisions allows near-quantitative description of the ultrafast hot-electron dynamics in a metal. Our calculations reveal the dominant role of the umklapp electron-phonon collisions. This is due to the fact that the phase space of the possible final electron states diminishes for normal processes and rises for umklapp collisions with increasing energy. The comparison of our results with the experimental results by Fann *et al.*[12] shows generally very good agreement. The occasional discrepancies are probably associated with the limited applicability of the relation (10) for the collision integral. This formula is valid if $\omega\tau_{e\text{-}e}\gg 1$ and $\omega\tau_{e\text{-}p}^{(0)}\gg 1$. In our case, $\omega\tau_{e\text{-}e}\approx 36$ and $\omega\tau_{e\text{-}p}^{(0)}\approx 3$ at $\epsilon_{\mathbf{k}}=\epsilon_F+\hbar\omega$. Figures 6 and 7 show better agreement with experiment for lower hot-electron energies where $\omega\tau_{e\text{-}p}^{(0)}$ is higher.

We find most interesting the result that the calculated electron-phonon collision rate is higher than the electron-electron scattering rate in the energy region where ''above threshold ionization electrons'' have been detected (Fig. 4). This means that in this energy region the hot-electron excitation in *e-p* collisions cannot be balanced by the *e-e* relaxation if the laser field is sufficiently high. Detailed study of this energy regime is currently under investigation.

*Electronic address: Andrey.Lugovskoy@flinders.edu.au

[1] H. Petek and S. Ogawa, Prog. Surf. Sci. **56**, 239 (1997).
[2] A. Othonos, J. Appl. Phys. **83**, 1789 (1998).
[3] F. Rossi, Semicond. Sci. Technol. **13**, 147 (1998).
[4] J. Z. Zhang, Acc. Chem. Res. **30**, 423 (1997).
[5] C. B. Harris, N. H. Ge, R. L. Lingle, J. D. Mcneill, and C. M. Wong, Annu. Rev. Phys. Chem. **48**, 711 (1997).
[6] R. W. Schoenlein, W. Z. Lin, J. G. Fujimoto, and G. L. Easley, Phys. Rev. Lett. **58**, 1680 (1987).
[7] C. Suarez, W. E. Bron, and T. Juhasz, Phys. Rev. Lett. **75**, 4536 (1995).
[8] R. H. M. Groeneveld, R. Sprik, and A. Lagendijk, Phys. Rev. B **45**, 5079 (1992).
[9] J. M. Hicks, L. E. Urbach, E. W. Plummer, and H.-L. Dai, Phys. Rev. Lett. **61**, 2588 (1988).
[10] J. Hohlfeld, U. Conrad, and E. Matthias, Appl. Phys. B: Lasers Opt. **63**, 541 (1996).
[11] W. S. Fann, R. Storz, H. W. K. Tom, and J. Bokor, Phys. Rev. Lett. **68**, 2834 (1992).
[12] W. S. Fann, R. Storz, H. W. K. Tom, and J. Bokor, Phys. Rev. B **46**, 13 592 (1992).
[13] M. I. Kaganov, I. M. Lifshitz, and L. V. Tanatarov, Zh. Éksp. Teor. Fiz. **31**, 232 (1956) [Sov. Phys. JETP **7**, 173 (1957)].
[14] S. I. Anisimov, B. L. Kapeliovich, and T. L. Perel'man, Zh. Éksp. Teor. Fiz. **66**, 776 (1974) [Sov. Phys. JETP **39**, 375 (1974)].
[15] R. H. M. Groeneveld, R. Sprik, and A. Lagendijk, Phys. Rev. B **51**, 11 433 (1995).
[16] C. K. Sun, F. Vallee, L. Acioli, E. P. Ippen, and J. G. Fujimoto, Phys. Rev. B **48**, 12 365 (1993).
[17] S. Ogawa, H. Nagano, and H. Petek, Phys. Rev. B **55**, 10 869 (1997).
[18] E. Knoesel, A. Hotzel, and M. Wolf, Phys. Rev. B **57**, 12 812 (1998).
[19] J. Cao, Y. Gao, R. J. Miller, H. E. Elsayed-Ali, and D. A. Mantell, Phys. Rev. B **56**, 1099 (1997).
[20] S. Luan, R. Hippler, H. Schwier, and H. O. Lutz, Europhys. Lett. **9**, 489 (1989).
[21] G. Farkas, C. Toth, and A. Kohazi-Kis, Opt. Eng. (Bellingham) **32**, 2476 (1993).
[22] G. Farkas, C. Toth, A. Kohazi-Kis, P. Agostini, G. Petite, P. Martin, J. M. Bersett, and J. M. Ortega, J. Phys. B **31**, L461 (1998).
[23] R. N. Gurzhi, Zh. Éksp. Teor. Fiz. **33**, 451 (1957) [Sov. Phys. JETP **6**, 451 (1958)].
[24] R. N. Gurzhi, Zh. Éksp. Teor. Fiz. **33**, 660 (1957) [Sov. Phys. JETP **6**, 506 (1958)].
[25] V. I. Mel'nikov, Pis'ma Zh. Éksp. Teor. Fiz. **9**, 204 (1969) [JETP Lett. **9**, 120 (1969)].
[26] E. M. Epshtein, G. M. Shmelev, and G. I. Tsurkan, *Photostimulated processes in semiconductors* (Stiintsa, Kishinev, 1987) (in Russian).
[27] A. V. Lugovskoy, T. Usmanov, and A. V. Zinoviev, J. Opt. Soc. Am. B **15**, 53 (1998).
[28] A. V. Zinov'ev and V. B. Lugovskoi, Zh. Tekh. Fiz. **50**, 1635 (1980) [Sov. Phys. Tech. Phys. **25**, 953 (1980)].
[29] A. V. Lugovskoy, T. Usmanov, and A. V. Zinoviev, J. Phys. D **27**, 628 (1994).
[30] C. K. Sun, F. Vallee, L. Acioli, E. P. Ippen, and J. G. Fujimoto, Phys. Rev. B **50**, 15 337 (1994).
[31] D. Bejan and G. Raşeev, Phys. Rev. B **55**, 4250 (1997).
[32] V. E. Gusev and O. B. Wright, Phys. Rev. B **57**, 2878 (1998).
[33] D. V. Volkov, Z. Phys. **56**, 250 (1935).
[34] R. Potvliege and R. Shakeshaft, in *Atoms in Intense Laser Fields*, [Adv. At. Mol. Opt. Phys. Supp. 1] (Academic Press, San Diego, CA, 1992), Vol. XVII, p. 373.
[35] F. V. Bunkin and M. V. Fedorov, Zh. Éksp. Teor. Fiz. **49**, 1215 (1965) [Sov. Phys. JETP **22**, 844 (1966)].
[36] N. L. Manakov, V. D. Ovsyannikov, and L. P. Rapoport, Phys. Rep. **141**, 319 (1990).
[37] A. L'Huillier, L.-A. Lompre, G. Mainfray, and C. Manus, in *Atoms in Intense Laser Fields* (Ref. 34), p. 139.
[38] D. K. Wagner and R. Bowers, Ann. Phys. (N.Y.) **27**, 651 (1978).
[39] M. Aeschlimann, M. Bauer, and S. Pawlik, Chem. Phys. **205**, 127 (1996).
[40] V. A. Gasparov and R. Huguenin, Ann. Phys. (N.Y.) **42**, 394 (1993).
[41] A. Lugovskoy and I. Bray, J. Phys. D **31**, L78 (1998).
[42] N. W. Ashcroft and N. D. Mermin, *Solid State Physics* (Holt, Rinehart and Winston, New York, 1976).
[43] B. P. Barua and S. K. Sinha, J. Appl. Phys. **49**, 3967 (1978).
[44] M. V. Fedorov, *Interaction of Intense Laser Light with Free Electrons*, edited by V. S. Letokhov, *Laser Science and Technology, an International Handbook* Vol. 13 (Harwood Academic,

Chur, Switzerland, 1991).
[45] P. B. Allen, Phys. Rev. Lett. **59**, 1460 (1987).
[46] W. L. McMillan, Phys. Rev. **167**, 331 (1968).
[47] J. P. Girardeau-Montaut and C. Girardeau-Montaut, Phys. Rev. B **51**, 13 560 (1995).
[48] O. Madelung, *Introduction to Solid-State Theory*, edited by M. Cardona, P. Fulde, and H.-J. Queisser, Springer Series in Solid-State Sciences Vol. 2 (Springer, Berlin, 1978).